A Parametric Study of Planform Effects on Rotor Hover Performance Using a Hybrid Navier Stokes – Free Wake Methodology

Jeewoong Kim and Lakshmi N. Sankar
School of Aerospace Engineering, Georgia Tech, Atlanta, GA, USA

Ritu Marpu
CD-adapco, Orlando, FL, USA

T. Alan Egolf
Sikorsky Aircraft Corporation, Bridgeport, CT, USA

Nathan Hariharan
HPCMP, CREATE-AV, Lorton, VA

Abstract

A hybrid Navier-Stokes/Free Wake methodology is applied to helicopter rotors in hover. Three tip planforms were analyzed: the S-76 rotor with a swept tip, a rectangular planform, and a swept tip with anhedral. The solidity of the three rotors was matched. A pitch sweep was conducted. Computed thrust, power, and figure of merit values have been compared with test data. Where available, comparisons with other calculations for these quantities and the near wake tip vortex trajectory have been done. The simulations are in reasonable agreement with published data for the thrust, power, and figure of merit. The simulations differ from full Navier-Stokes calculations in the predictions for tip vortex descent rate and contraction rate. The simulations correctly predicted the trends. The swept tapered anhedral tip had the highest figure of merit, followed by the swept tapered tip. The rectangular planform had the lowest figure of merit.

1. Introduction

Over the past three decades, significant progress has been made in the modeling of rotors in hover. A variety of approaches have been developed. These include fixed and free wake models, structured and unstructured Navier-Stokes analyses, potential flow solvers with embedded vorticity fields, and hybrid Navier-Stokes-free wake analyses. The present authors have recently conducted a brief survey of many of these techniques[1]. Much of the published has been for classical rectangular blade rotors of low aspect ratios[2], or for a scaled model of a representative rotor such as the UH-60A[3]. A limited amount of test data is available for modern rotors such as the S-76, with parametric studies of the effects of tip planform on hover performance[4,5]. This valuable set of data has not yet been used to assess the current state of the art in hover prediction methodology.

The present authors, under the charter of the AIAA Applied Aerodynamics Technical Committee, have assembled a Rotorcraft Simulation Working Group comprising of researchers around the world with the immediate purpose of assessing current state-of-the-art in hover prediction methodology \, determining critical challenges in consistently and accurately predicting hover performance, and serving as a leading catalyst in the development of computational methods for solving rotorcraft problems.

There were several challenges in setting up a common rotor-in-hover test case to enable a workshop and get different participants to predict hover performance using their codes. These included obtaining a publicly available realistic geometry with reliable force balance, surface pressure tap, and PIV data, and complications due to blade aero-elastic deformations. The team discussed several candidate existing benchmark cases including the UH60A model rotor, HART rotor, Comanche rotor, and S-76. Although pressure and visualization data are not available, it was concluded that the S-76, because of its linear twist, and publicly available notional section geometry, and planform, was the best candidate for a systematic evaluation of the capabilities and gaps of current generation of codes. For the first round of comparisons, the effect of aeroelastic deformation was not considered. A representative S-76 blade geometry, with built-in aeroelastic deformations for a representative loading configuration was provided to all potential participants.

An invited session was organized at the AIAA SciTech 2014 Conference. This session was limited to the baseline S-76 computations, with tip-shape effects deferred for future workshops. The participants included Georgia Tech in collaboration with Sikorsky[6], Boeing Helicopters[7,8], University of Maryland[9], University of Toledo[10], US Army AeroFlightDynamics Directorate[11], University of Liverpool[12], and KAIST[13].

2. Research Objectives

In the present work, we extend the earlier work reported in Ref. 6. A comparison of the present methodology with other published computational data is first presented for the baseline S-76 planform. Subsequently, two other tip shapes are modeled: a rectangular planform, and a swept-tapered tip with anhedral. Figure 1 shows the planforms that are being modeled. Note that the 35 degree leading edge sweep is a 20 degree sweep of the ¼ chord line.

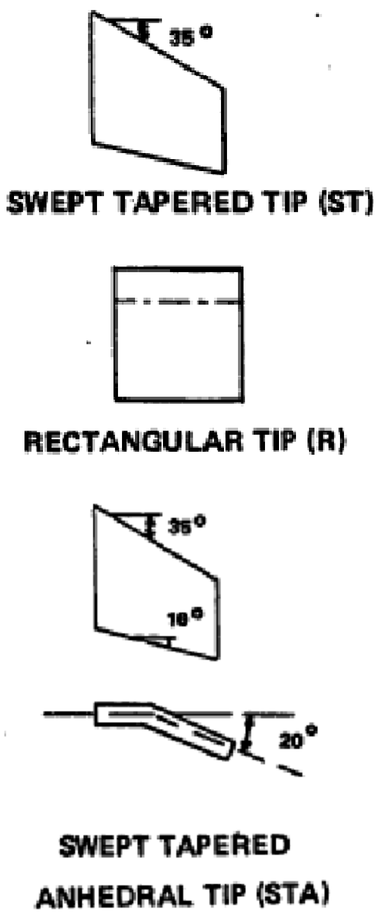

Figure 1. Planforms being Modeled[4,5].

3. Grid Generation

The S-76 blades are 1/4.71 scale and possess a -I0° linear twist and a solidity σ of .0704. The blades have a radius of 1.423m (56.04 in.), a chord of .0787m (3.1 in.) and use the SC1095 and SCI094 R8 airfoils. A refined C-H grid with 291 points in the wrap-around direction, 98 radial grid points on the blade, and 45 points in the normal direction was generated using an in-house grid generator. The model provided, and modeled, both had a blunt open tip. The surface grid for the baseline S-76 rotor has been placed on the APA Rotor Simulation Working Group share-point site[14].

The same grid generator was used to generate the surface and volume grids for the rectangular tip blade, and the blade with swept-tapered-anhedral tip. It was necessary only to modify the input data set that specifies the blade planform (leading edge x, y, z at several radial locations; section airfoil coordinates; blade chord; twist). The total number of points in each of the three directions was kept the same. The grid clustering in the leading and trailing edge regions as well as the normal grid spacing and stretching factors were all kept identical for the three planforms.

4. CFD Solution Methodology

The CFD methodology used in this study is a 3-D finite volume based three-dimensional unsteady viscous compressible flow solver called GT-Hybrid, described in Ref. 15-18. This analysis performs the costly Navier-Stokes calculations only in the immediate vicinity of the rotor blades. Away from the rotor, the vortex wake is captured using a Lagrangean approach. This hybrid approach allows for an accurate and economical modeling of viscous features near the blades, and an accurate "non-diffusive" modeling of the trailing wake in the far field. Figure 2 shows a schematic of the Hybrid method employed in GT-Hybrid, depicting the Navier-Stokes domain around the blade-region, the wake captured inside the near-blade Navier-Stokes domain, and the portion of the wake which is modeled as a Lagrangian free wake.

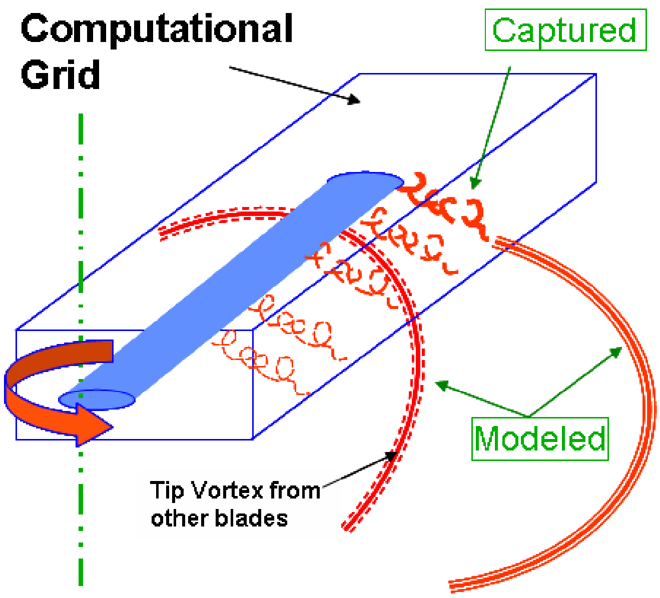

Figure 2. A Schematic View of the Hybrid Method.

The influence of the trailed vortices from the wake model on the blade aerodynamics is computed by appropriately specifying the vortex-induced velocities at the far field boundary of the Navier-Stokes domain, neglecting the contribution of the elements captured within the CFD volume grid.

5. Run Settings

The present researchers conducted simulations for the S-76 rotor in hover for a collective sweep of 4 to 12 degrees by increments of 1 degree. One condition trimmed to C_T/σ=0.09 at a nominal tip Mach number of 0.65 was also done. The tip Reynolds (Retip) number based on chord length is 1.332 Million.

The simulations were done using a Linux Cluster with 12 CPU cores. The wall clock time was approximately 7 to 8 hours per collective pitch setting. On a 72 core cluster available to the present investigators, the entire performance map may be generated overnight, if desired. The output from the present analyses may also be passed onto computational structural dynamics analyses, icing analyses, and aeroacoustics analyses as desired. Thus, the present methodology allows a rapid and efficient physics based screening of planform effects from a multi-physics perspective, prior to the use of potentially more accurate full Navier-Stokes methodologies.

The following results were generated:

1) Plots of the thrust coefficient C_T and the torque coefficient C_Q versus collective pitch, plots of C_Q versus C_T, and plots of figure of merit FM versus C_T.
2) Section thrust and torque coefficients, as a function of radial position r/R. The section thrust coefficient is defined as: $(dT/dr)/(1/2\rho c(\Omega r)^2)$ and the section torque coefficient is defined as: $(dQ/dr)/(1/2\rho cR(\Omega r)^2)$. Here c is the local chord, dT/dr is the thrust per unit span, and dQ/dr is the torque per unit span.
3) Pressure distributions as sectional chordwise plots of C_p versus x/c where C_p is defined as $(p-p_\infty)/(1/2\rho c(\Omega r)^2)$ for the following radial stations (r/R): 0.20, 0.40, 0.60, 0.70, 0.75, 0.80, 0.85, 0.90, 0.925, 0.95, 0.975, 0.99.
4) Tip vortex trajectory as a function of wake age. The tip vortex descent rate and contraction rate were examined.

For brevity, only a small subset of the simulations are shown and discussed in this work.

6. Results and Discussions

Prior to the simulations, the available experimental data was examined. In hover, the most important quantity is the figure of merit, FM. Its variation with thrust over the operating range is of particular interest. Figure 3 shows FM vs C_T/σ for several tip shapes. The test data indicate that the unswept tip begins to pay a penalty at higher tip Mach numbers (0.65 in the present case) due to the onset of shock waves. The straight tapered blade is more efficient at lower thrust settings. As thrust setting increases, its performance diminishes due to transonic effects, relative to swept tips. The swept tapered tip with anhedral performs significantly better than all the other planforms over the entire range.

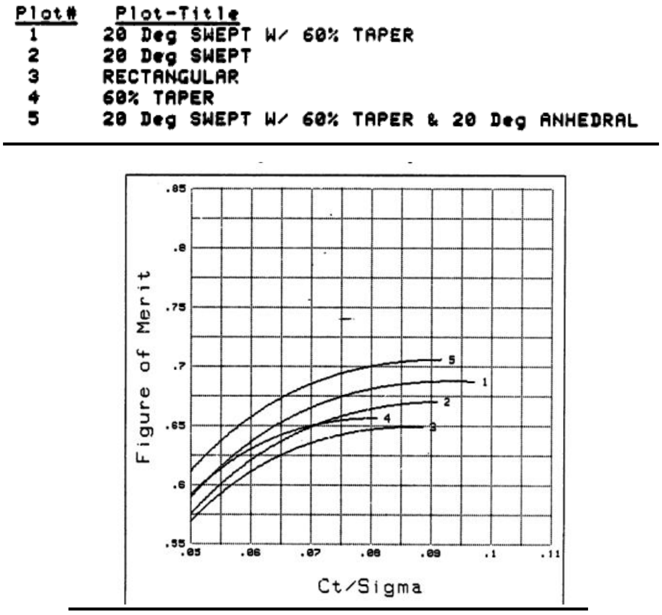

Figure 3 Measured Figure of Merit Data for Various Planforms at M_{tip}=0.65[4, 5].

Baseline S-76 Rotor

The variation of CT with the collective pitch is shown in Figure 4 below for a rotational tip Mach No of 0.65. In addition to the present work, several other Navier-Stokes simulations are also shown. Test data is also presented. It should be noted the data for other Navier-Stokes simulations were extracted by digitizing their plots, and there may be minor discrepancies attributable to the digitization process. It is seen that all the computed data are in good agreement with each other. At higher pitch settings, GT-Hybrid has a tendency to slightly over predict the thrust coefficient.

Figure 5 shows the variation of torque coefficient with pitch. It must be noted that there has been no attempt to use comparable grids or identical turbulence models. The methodologies have other differences with each other such as structured vs. unstructured, single block vs. overset, central vs. upwind, etc. Keeping these differences in mind, it is seen that OVERFLOW and GT-Hybrid tend to over predict the torque coefficient. The other analyses (Helios, OVERTURNS simulations done at University of Maryland, and the simulations done at KAIST) gave very favorable agreement with test data.

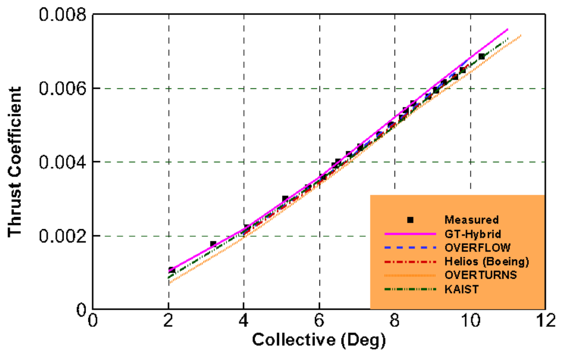

Figure 4. Variation of Thrust Coefficient with Pitch, Baseline S-76 Configuration.

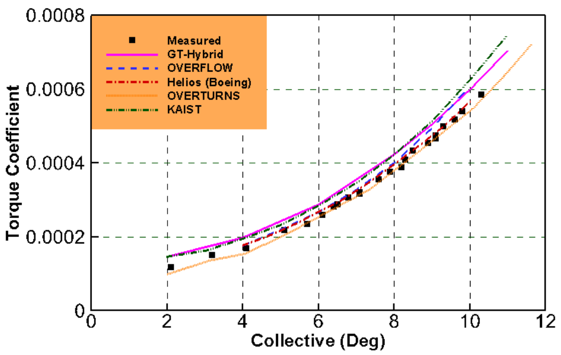

Figure 5. Variation of Torque Coefficient with Pitch, Baseline S-76 Configuration.

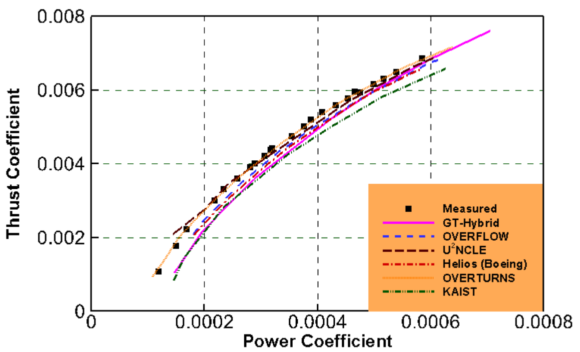

Figure 6. Variation of Thrust vs Torque Coefficient, Baseline S-76 Configuration.

In vehicle performance, the thrust vs torque curve is of particular interest. The data shown in figures 4 and 5 have been plotted as CT vs CQ plot in Figure 6.

In this case, OVERTURNS and U^{2}NCLE gave the best correlation with test data. All other simulations, including GT-Hybrid, tended to over predict the torque coefficient for a given thrust setting. This tendency to over predict the power (or torque) for a given level of thrust leads to an under prediction of the figure of merit in most of the calculations including GT-Hybrid. In Figure 7, it is seen that only the OVERTURNS and U^{2}NCLE gave satisfactory results.

The hover performance is strongly influenced by rotor inflow, which in turn is influenced by the tip vortex trajectory. Figure 8 shows the tip vortex descent rate and contraction rate as a function of vortex age. There are no test data available. OVERTURNS and U2NCLE gave a slightly larger descent rate than the other methodologies. The present GT-Hybrid method uses a free vortex (Lagrangian) method in the near field with a far field trajectory model based on fitting the behavior at a specified wake age while all the other methods use a vortex capturing (Eulerian) method. As a result, good correlation between the present method and others could only be achieved for the first revolution, 360 degrees of vortex age, when the vortex is coherent with a very small vortex core radius. At higher vortex age, factors such as numerical diffusion, grid density, etc begin to cause deviations among the various methods. It was also observed that the GT-Hybrid methodology significantly underestimated the tip vortex contraction rate at higher wake ages, compared to other methods.

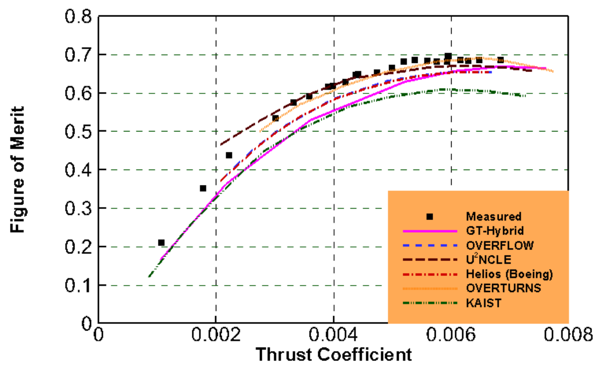

Figure 7. Variation of Figure of Merit with Thrust Coefficient, Baseline S-76 Configuration.

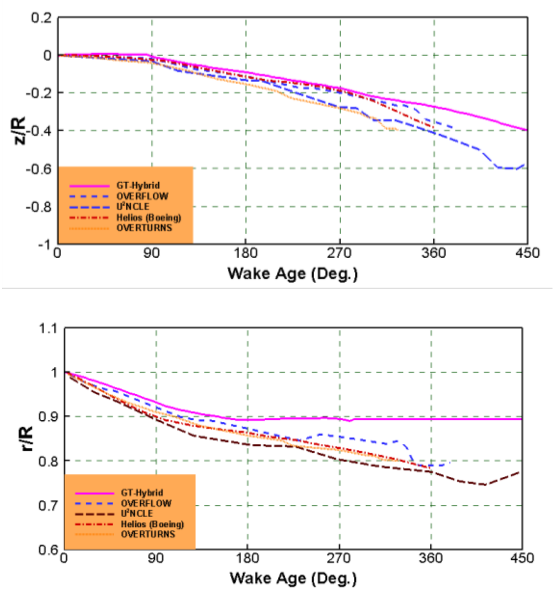

Figure 8. Computed Tip Vortex descent rate and Contraction Rate for Baseline case (C_T/σ=0.09).

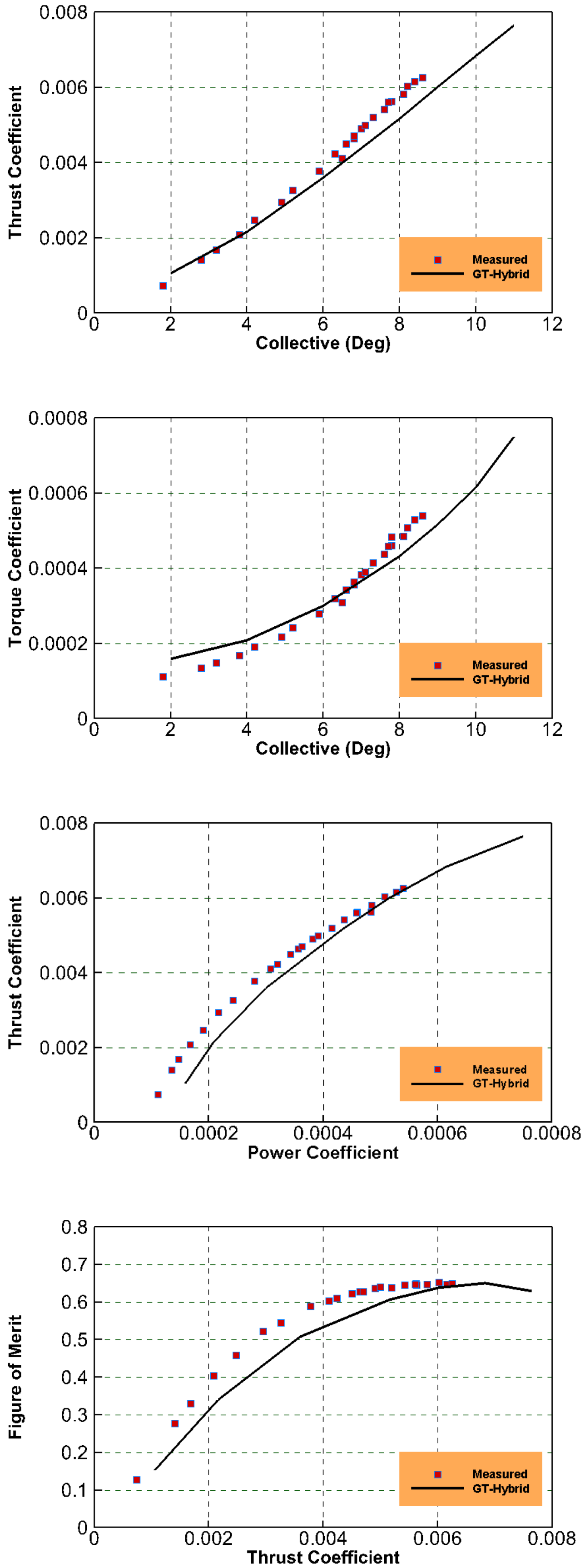

Figure 9. Hover Performance Characteristics of the Rectangular Planform.

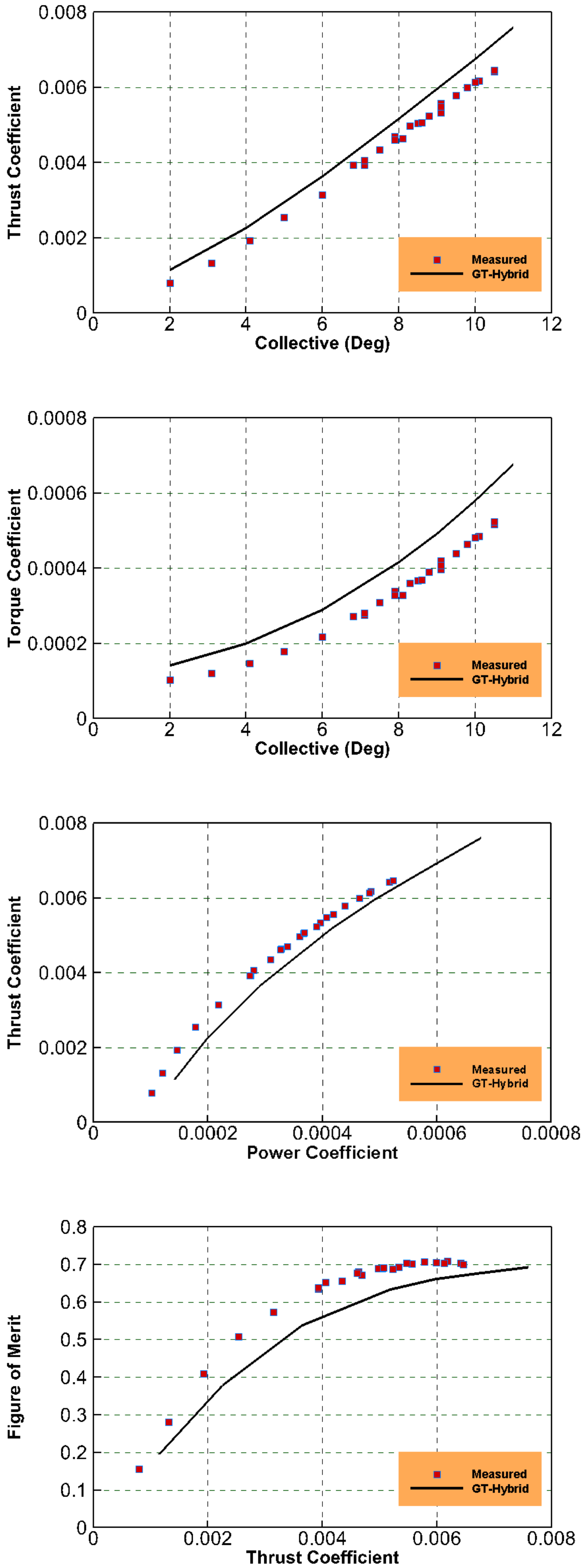

Figure 10. Hover Performance Characteristics of the Swept, Tapered, Anhedral Planform.

Tip Variations

Figure 9 and 10 show the hover performance for the rectangular planform, and for the swept-tapered-anhedral planform respectively. As stated earlier, these configurations were analyzed using comparable grids to the baseline configuration, with the same turbulence model (Spalart-Almaras). The grid was constructed one span station at a time, and assembled into the 3-D volume grid. Thus, there will be grid slope discontinuities at the radial locations where the taper/sweep and anhedral effects begin. No attempt has been made at this writing to smooth the grid using a technique such as elliptic smoothing. As seen earlier for the baseline case, torque was overestimated for a given thrust setting, for both the rectangular and the swept-tapered-anhedral configuration, leading to lower figure of merit. Nevertheless, the calculations begin to correctly predict the improvement in the figure of merit attributable to the anhedral effects as shown in Figure 11 for the measured results and Figure 12 for the calculations

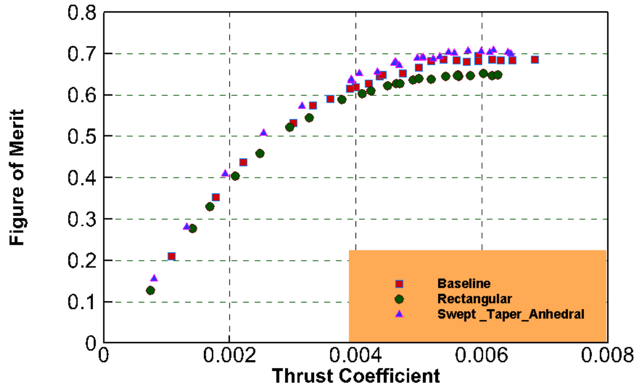

Figure 11a. Effects of Planform on Figure of Merit. (Measured)

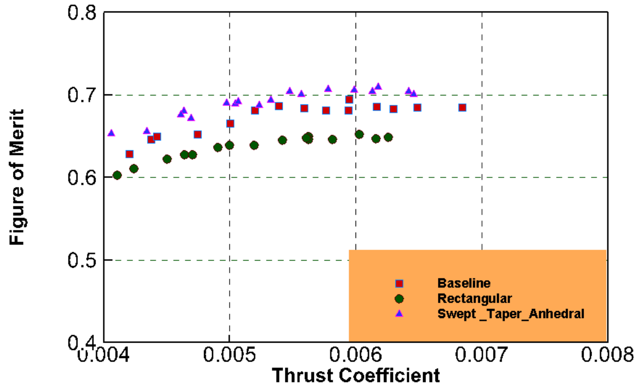

Figure 11b. Effects of Planform on Figure of Merit (Measured), Enlarged View.

Figure 11a shows the effects of planform on figure of merit for the full range of thrust studies. For clarity, an enlarged view of the same graph is shown at the higher thrust settings of primary interest in Figure 11b. As stated earlier (Figure 3), the swept-tapered-anhedral tip performs the best. The baseline S-76 with sweep and taper is the second best candidate. The rectangular planform performs progressively poorly as thrust setting increases.

Figure 12a and 12b (expanded view at higher thrust settings) correctly capture the trends observed in test data. While the figure of merit values, in all cases, are under predicted, the trends are consistent with test data, and indicate progressive improvement in performance progressing from the rectangular planform to the swept tapered planform to the swept-tapered-anhedral tip. Surface pressure data have also been computed and tabulated for all of these cases, and are available for one to one comparison with other methodologies.

To understand the improved performance of the baseline rotor and the rotor with the swept-tapered-anhedral tip over the rectangular planform, surface pressure contours, and spanwise loading have been examined for a representative pitch setting of 9 degrees. The sweep and the taper both tend to reduce the tip loading, tip vortex strength, and the associated induced drag, induced torque, and power as shown Figure 13. The reduction in the wetted area relative to the rectangular planform also has a small effect on the profile power. These factors collectively influence the figure of merit as seen in Figure 12b.

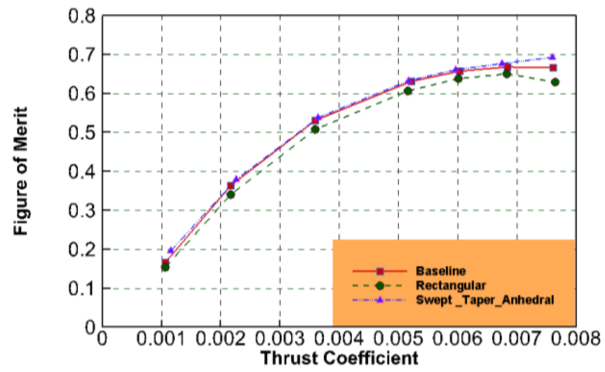

Figure 12a. Effects of Planform on Figure of Merit. (Computed)

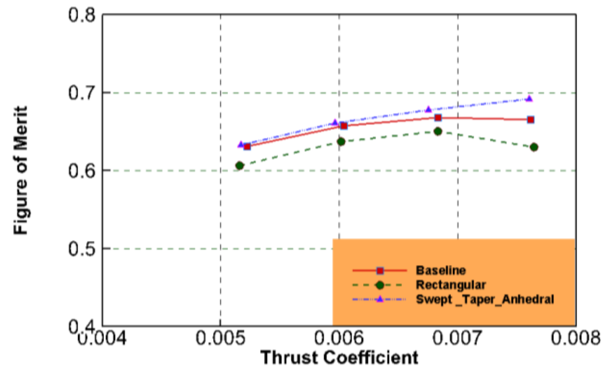

Figure 12b. Effects of Planform on Figure of Merit (Computed), Enlarged View.

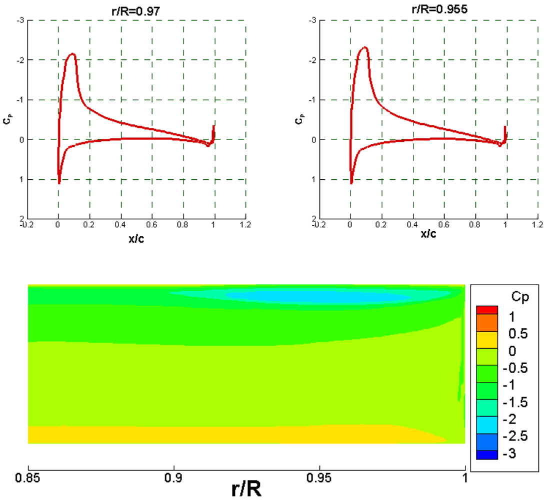

Rectangular Planform

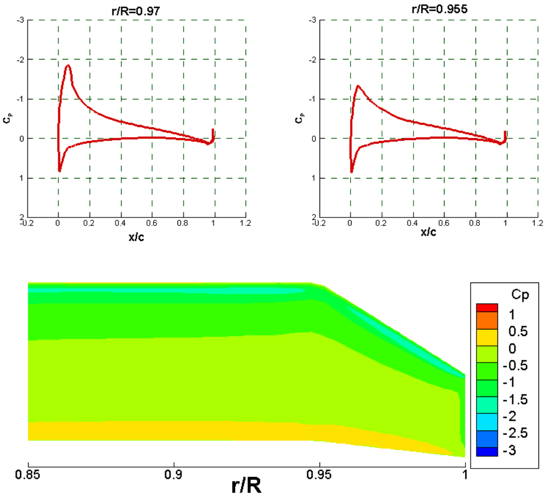

Swept, Tapered, Anhedral Planform

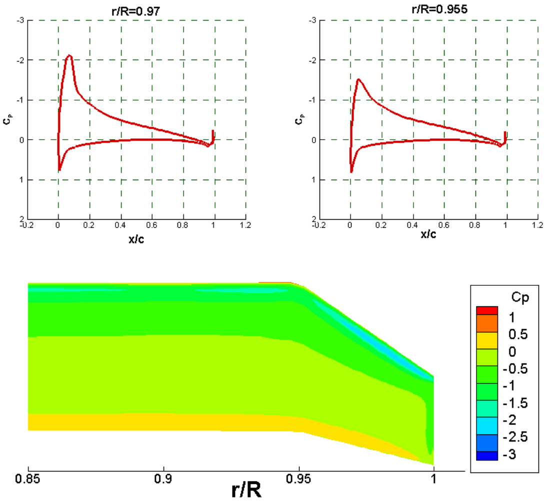

Swept, Tapered Planform

Figure 13a. Upper Surface Pressure Contours.

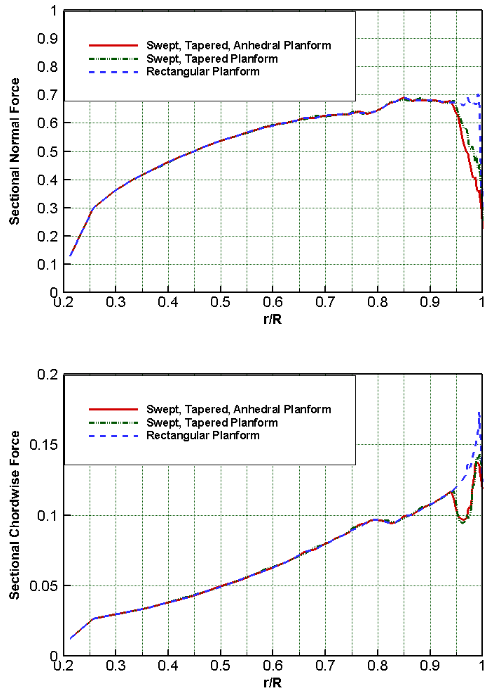

Figure 13b. Radial variation of Normal and Chordwise Forces at 9° Collective Pitch.

The tip vortex geometries have also been examined for the three planforms at a collective pitch of 9 degrees. The vertical descent rate and radial contraction rates as a function of the vortex age are shown in Figure 14. It must be emphasized that these calculations are based on the Lagrangian discretized representation of the tip vortex. No comparisons with other simulations have been conducted at this writing.

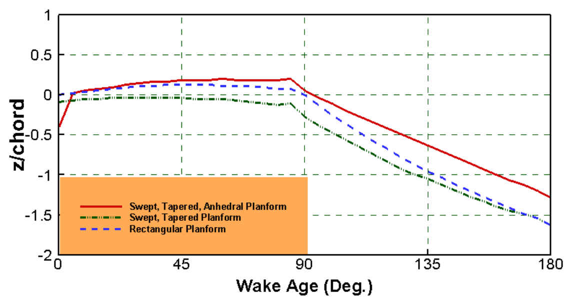

Figure 14a. Tip Vortex Descent Rate, 9 Degree Collective Pitch.

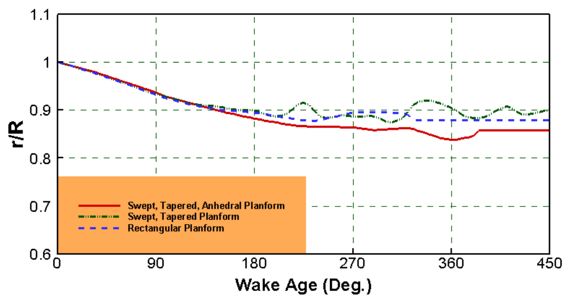

Figure 14b. Tip Vortex Contraction Rate, 9 Degree Collective Pitch.

4. Summary and Recommendations

Hover performance calculations have been done for three planforms representative of modern helicopter rotors. Comparisons with other numerical data and experimental data have been made. The present methodology, like several other methods, tended to overestimate the power setting for a given thrust setting, leading to an underestimate of the figure of merit. However, the trends in the performance as the planform is progressively modified were correctly modeled. Additional work is needed to improve the present methodology. This approach, because of its efficient modeling of the wake structure using Lagrangean methods and reduced computer time, may be used in its present form by the designers to explore design trends.

Acknowledgments

Part of material presented in this paper is a product of the HPCMP CREATE-AV Element of the Computational Research and Engineering for Acquisition Tools and Environments (CREATE) Program sponsored by the U.S. Department of Defense HPC Modernization Program Office. Dr. Robert Meakin is the program manager for CREATE-AV.

REFERENCES

[1] Hariharan, N., Egolf, T. A., and Sankar, L. N., "Simulation of Rotor in Hover: Current State, Challenges and Standardized Evaluation," AIAA 2014-0041.

[2] Caradonna, F.X., and Tung, C., "Experimental and Analytical Studies of a Model Helicopter Rotor in Hover," NASA TM 81232, 1981.

[3] Lorber, P.F., et al., "A Comprehensive Hover Test of the Airloads and Airflow of an Extensively Instrumented Model Helicopter Rotor," Proceedings of the 45th Annual Forum, American Helicopter Society, May 1989, pp 281-295.

[4] Balch, D. T., "Experimental Study of Main Rotor Tip Geometry and Tail Rotor Interactions in Hover, Volume 1, Test and Figures," NASA CR 177336, 1985.

[5] Balch, D. T., "Experimental Study of Main Rotor Tip Geometry and Tail Rotor Interactions in Hover, Volume 2, Run Log and Tabulated Data," NASA CR 177336, 1985.

[6] Marpu, R., Sankar, L. N., Egolf, T. A., and Hariharan, N., "Simulation of S-76 Rotor in Hover Using a Hybrid Methodology," AIAA-2014-0210, SciTech 2014, January 2014.

[7] Tadghighi, Hormoz, "Simulations of Rotor in Hover: Boeing Mesa," AIAA-2014-0209, SciTech 2014, National Harbor, MD, January 2014.

[8] Narducci, Robert, "Simulations of Rotor in Hover: Boeing Philadelphia," AIAA-2014-0208, SciTech 2014, National Harbor, MD, January 2014.

[9] Baeder, J., Medida, S., "OVERTURNS Simulation of S-76 Rotor in Hover," AIAA-2014-0045, SciTech 2014, National Harbor, MD, January 2014.

[10] Sheng, C., Zhao, Q., Wang, J., "S-76 Rotor Hover Prediction Using U2NCLE Solver," AIAA 2014-0044, SciTech 2014, January 2014.

[11] Jain, R. K., and Potsdam, M., "Hover Predictions on the Sikorsky S-76 Rotor using Helios," AIAA 2014-0207, SciTech 2014, January 2014.

[12] Barakos, George N., "Evaluating Rotor Tip Shapes Using Computational Fluid Dynamics," AIAA-2014-0043, SciTech 2014, National Harbor, MD, January 2014.

[13] Jung, M. K., Hwang, J. Y., and Kwon, O. J., "Assessment of Rotor Aerodynamic Performance in Hover Using an Unstructured Mixed Mesh Method," AIAA_2014-0042, SciTech 2014, National Harbor, MD, January 2014.

[14] AIAA Applied Aero Rotorcraft Working Group, https://info.aiaa.org/tac/ASG/APATC/Web%20Pages/RotorSim-DG_Info.aspx

[15] Rajmohan, N., "Application of Hybrid Methodology to Rotors in Steady and Maneuvering Flight", Ph.D. Dissertation, Georgia Institute of Technology, 2010.

[16] Rajmohan N., Sankar L.N., Costello M., "Effect of Inflow Model on Coupling between Aeromechanics and Flight Mechanics", 49th AIAA Aerospace Sciences Meeting, Orlando, Florida, Jan 2011.

[17] Marpu R., Sankar L.N., Stephen Makinen., Baeder J.D., "Computational Modeling of Diving-turn Maneuvers using Hybrid Methodology," AHS 68th Annual Forum, Fort Worth, TX, 2012

[18] Marpu R. P., Sankar L.N., Makinen S., Egolf T.A., Baeder J.D. and Wasikowski, M., "Physics Based Modeling of Maneuver Loads for Rotor and Hub Design," Journal of Aircraft, 2014, Vol, 51: 377-389, 10.2514/1.C031843.

COPYRIGHT STATEMENT